IOPscience iopscience.iop.org

Home Search Collections Journals About Contact us My IOPscience

On the use of peripheral autonomic signals for binary control of body–machine interfaces

This article has been downloaded from IOPscience. Please scroll down to see the full text article.

2010 Physiol. Meas. 31 1411

(http://iopscience.iop.org/0967-3334/31/11/001)

View the table of contents for this issue, or go to the journal homepage for more

Download details:
IP Address: 130.15.19.60
The article was downloaded on 22/09/2010 at 19:11

Please note that terms and conditions apply.

IOP PUBLISHING PHYSIOLOGICAL MEASUREMENT

Physiol. Meas. **31** (2010) 1411–1422 doi:10.1088/0967-3334/31/11/001

On the use of peripheral autonomic signals for binary control of body–machine interfaces

Tiago H Falk[1,2], **Mirna Guirgis**[1], **Sarah Power**[1,2], **Stefanie Blain**[1,2] **and Tom Chau**[1,2,3]

[1] Bloorview Research Institute, Holland Bloorview Kids Rehabilitation Hospital, Toronto, Canada
[2] Institute of Biomaterials and Biomedical Engineering, University of Toronto, Toronto, Canada

E-mail: tom.chau@utoronto.ca

Received 1 February 2010, accepted for publication 2 August 2010
Published 10 September 2010
Online at stacks.iop.org/PM/31/1411

Abstract

In this work, the potential of using peripheral autonomic (PA) responses as control signals for body–machine interfaces that require no physical movement was investigated. Electrodermal activity, skin temperature, heart rate and respiration rate were collected from six participants and hidden Markov models (HMMs) were used to automatically detect when a subject was performing music imagery as opposed to being at rest. Experiments were performed under controlled silent conditions as well as in the presence of continuous and startle (e.g. door slamming) ambient noise. By developing subject-specific HMMs, music imagery was detected under silent conditions with the average sensitivity and specificity of 94.2% and 93.3%, respectively. In the presence of startle noise stimuli, the system sensitivity and specificity levels of 78.8% and 80.2% were attained, respectively. In environments corrupted by continuous ambient *and* startle noise, the system specificity further decreased to 75.9%. To improve the system robustness against environmental noise, a startle noise detection and compensation strategy were proposed. Once in place, performance levels were shown to be comparable to those observed in silence. The obtained results suggest that PA signals, combined with HMMs, can be useful tools for the development of body–machine interfaces that allow individuals with severe motor impairments to communicate and/or to interact with their environment.

Keywords: body–machine interface, hidden Markov models, peripheral autonomic signals, music imagery, startle reflex

(Some figures in this article are in colour only in the electronic version)

[3] Author to whom any correspondence should be addressed.

 © 2010 Institute of Physics and Engineering in Medicine

1. Introduction

Physical disabilities often make extremely difficult or completely impossible for an individual to independently communicate or to interact with the surrounding environment. Access technologies, or *human–machine interfaces*, serve to translate user intentions into useful control signals. Representative technologies can include eye gaze (Sesin *et al* 2008), head (Chen 2001) and tongue control devices (Struijk 2006), gesture (Roy *et al* 1994) and speech recognition (Su and Chung 2001), as well devices based on residual muscle contractions (Alsayegh 2000). Such technologies, however, require volitional (residual) motor control, and hence are not applicable to individuals who posses no functional movement or speech as a result of e.g. degenerative motor neuron diseases, cerebral palsy, brain stem stroke or traumatic brain injuries. Such individuals are cognitively active but are 'locked' in a non-functional body. To this end, *brain–machine interfaces* (BMI) have emerged as promising solutions.

As the name suggests, BMI use the brain activity—harnessed via e.g. electroencephalography (EEG), electrocorticography (ECoG), functional magnetic resonance imaging (fMRI), magnetoencephalography (MEG) or near-infrared spectroscopy (NIRS)—to develop control signals for the machine interaction. As argued by van Gerven *et al* (2009), however, existing solutions require lengthy user training sessions and can cause premature user fatigue as significant mental effort is required to produce detectable brain signals. Additionally, the system performance can be severely affected from the interference caused by hair (e.g. with EEG- and NIRS-based technologies). These shortcomings can cause user frustration and lead to device abandonment (van Gerven *et al* 2009).

More recently, studies have shown that physiological signals can be volitionally controlled and used to translate functional intent into actions; such technologies have been termed *body–machine interfaces*. Promising systems have been proposed based on facial temperature changes (Memarian *et al* 2009), skin electrodermal activity (EDA), also known as the galvanic skin response (e.g. Blain *et al* 2006, Tsukahara and Aoki 2002), and salivary pH levels (Wilhelm *et al* 2006). Additionally, signals such as heart rate (HR), respiration rate (RR) and skin temperature (ST) have been previously explored for biofeedback and mental relaxation (Blain *et al* 2008a). Hence, such signals have the potential of serving as additional modalities for the development of body–machine interfaces.

The overarching goal of this study was to investigate the potential of using four non-invasively acquired peripheral autonomic (PA) signals, namely EDA, ST, HR and respiration, to automatically discriminate between two cognitive states. More specifically, the proposed system used hidden Markov models (HMMs) to distinguish between baseline (i.e. rest) and a higher cognitive state of music imagery (singing in one's head). Automated detection of music imagery can be used, for example, as a binary signal to control a body–machine interface.

Moreover, in order to develop technologies that can be taken beyond controlled scenarios and into everyday surroundings, the effects of environmental factors need to be ascertained. Previous studies have suggested, for example, that distracting auditory stimuli can have a detrimental effect on technologies based on PA signals (Cook *et al* 1991) due to involuntary startle-reflex responses. In light of this issue, we propose a simple startle noise detection and compensation scheme to suppress erroneous activations resultant from involuntary responses. The experiments described herein suggest that reliable system accuracy can be achieved under both silent and noisy conditions.

The remainder of this paper is organized as follows. Section 2 provides a description of the materials and methods used in the study. Experimental results are reported in section 3 for both silent and noisy environmental conditions. Lastly, conclusions are drawn in section 4.

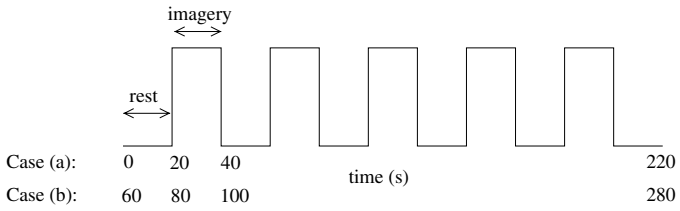

Figure 1. Stimulus pattern for the test imagery sessions. Reported time values are given for trials (a) without and (b) with an initial 60 s period for the user to habituate to the continuous ambient noise.

2. Materials and methods

2.1. Participants

Six adult participants (two males, four females) with a mean age of 28.1 ± 9.9 years participated in the study. Ethical approval was obtained from the affiliated institutes and the participants freely consented to participate. They were required to have normal hearing.

2.2. Protocol

The participants were involved in ten data collection sessions over a course of 2 days. Four sessions consisted of baseline trials, each 130 s in duration, with participants sitting at rest performing no mental task. The participants were instructed to focus on their breathing and to clear their minds. Half of these sessions were performed in a controlled silent environment and the other half in the presence of five randomly played startle stimuli. Noise stimuli were all approximately 800 ms in duration and their respective loudness intensities in decibel (dB) were dog barking (80 dB), glass breaking (91 dB), door slamming (83 dB), person coughing (79 dB) and sneezing (82 dB).

The remaining six sessions consisted of the participants alternating between rest (i.e. baseline) and music imagery tasks. Before each session, the participants were instructed to select a minimum of two songs of the same emotional valence to be used throughout the session. The participants were cued to start and stop music imagery with a light tap on the arm. Of these six sessions, two were performed in a controlled silent environment, two in the presence of five startle stimuli and two in the presence of combined continuous ambient noise (i.e. 'humming' of an air conditioner) *and* startle noises. Figure 1 depicts the stimulus pattern used. The last session involving continuous ambient noise lasted 280 s and consisted of an initial 60 s habituation period followed by alternating 20 s rest and imagery segments. For sessions under silent and startle noise conditions, this habituation period was not included; thus, those sessions lasted 220 s, as illustrated in figure 1. For all sessions, the participants sat comfortably on a desk and were equipped with four physiological signal sensors described in section 2.3.1.

2.3. System description

Figure 2 depicts the overall design of the proposed system. Four physiological signals, namely EDA, ST, HR and RR, were collected while the individual sat quietly at rest (baseline) and alternated between music imagery and rest (see section 2.2). Baseline data were used to train user-specific reference HMMs representative of the physiological response of the individual

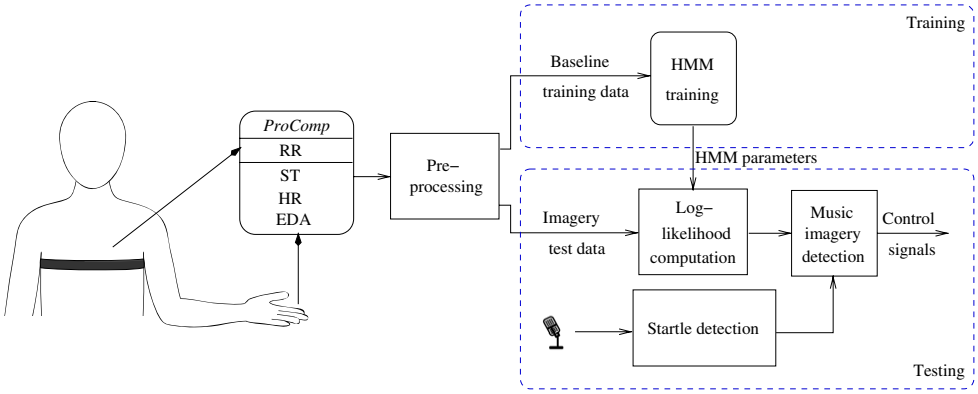

Figure 2. Overall design of the proposed interface. Four independent PA signals, namely EDA, ST, HR and RR, were measured and used to train subject-specific HMMs. Startle noise detection was used to improve the system performance in noisy environments.

at rest. Music imagery test data were scored against the reference HMMs via a log-likelihood measure and the obtained scores were used for automatic music imagery detection. A detailed description of each block is provided in the following subsections.

2.3.1. Physiological signal measurement and pre-processing. The four physiological signals were recorded simultaneously using a ProComp Infiniti multi-modality encoder (Thought Technology, Montreal, Canada) at a sampling frequency of 256 Hz. All sensors were placed on the non-dominant hand of the participant. EDA was measured from two 10 mm diameter Ag–AgCl surface electrodes attached to adhesive collars on the medial phalanges of the index and middle fingers. A constant 0.5 V was applied between the two electrodes. ST was measured using a thermal sensor on the distal phalange of the fifth finger. HR was computed from the interbeat intervals of the blood volume pressure waveform obtained with a photoplethysmograph sensor attached to the distal phalange of the fourth finger. Lastly, RR was measured by positioning a piezoelectric belt around the thoracic area; stretching due to expansion and contraction of the chest was converted into changes in voltage.

Signal pre-processing consisted of low-pass filtering for signal denoising. Fifth-order Butterworth filters with 0.2, 0.1, 1.2 and 0.3 Hz cutoff frequencies for EDA, ST, HR and RR, respectively, were used. The pre-processed PA signal temporal series were concatenated to form a K-dimensional feature vector $\mathbf{O}$, $K = 1, \ldots, 4$, where the time dependence has been omitted for notation simplicity. Feature vectors were subsequently used to train statistical models of physiological responses of the individuals at rest.

2.3.2. PA signal combination. In order to quantify the contribution of each PA signal, a normalized mutual information measure I_{norm} was used. Normalized mutual information is given by Kvalseth (1987):

$$\begin{aligned} I_{\text{norm}}(X_i, Y) &= \frac{2I(X_i, Y)}{H(X_i) + H(Y)} \\ &= \frac{2(H(X_i) + H(Y) - H(X_i, Y))}{H(X_i) + H(Y)} \\ &= 2 - \frac{2H(X_i, Y)}{H(X_i) + H(Y)}, \end{aligned} \tag{1}$$

where $H(\cdot)$ denotes the marginal entropy and $H(X_i, Y)$ the joint entropy between X_i and Y. In this study, X_i denotes each individual PA signal, $i = 1, \ldots, 4$, and Y the stimulus pattern depicted in figure 1. The signal with I_{norm} closest to unity represents the signal over which the user had the greatest volitional control; such a signal should contribute the most towards the imagery detection task at hand.

2.3.3. Hidden Markov models. HMMs, trained on the four collected physiological signals, were used to model the physiological response of the individual at rest. It was hypothesized that during cognitive tasks such as music imagery, physiological signals would undergo changes that deviated from this baseline response and such changes could be detected by means of a log-likelihood measure. Here, we use HMMs to capture the complex temporal signal interactions that arise once the user initiates the cognitive task. HMMs have been extensively used in the past for applications such as speech recognition and brain–computer interfaces, and hence are only briefly described here. The reader is referred to Rabiner (1989) for a detailed description.

HMMs represent a Markovian process with observable outputs being driven by the unobservable (hidden) states. To establish some notation, let Q be the number of states in the HMM and q_t indicate the state of the HMM at the time t. As such, an HMM can be completely characterized by three parameters $\boldsymbol{\lambda} = \{\boldsymbol{\pi}, \mathbf{A}, \mathbf{B}\}$, where

- $\boldsymbol{\pi} = \{\pi_1, \ldots, \pi_Q\}$ is the initial state distribution with $\pi_j = Pr(q_0 = j)$,
- $\mathbf{A} = \{a_{i,j}\}$ is the transition matrix with $a_{i,j} = Pr(q_t = j | q_{t-1} = i)$ describing the probabilities of transitioning from the state q_i to the state q_j, $1 \leqslant i, j \leqslant Q$, and
- $\mathbf{B}= \{b_j(\mathbf{O})\}$ is the observation probability distribution with $b_j(\mathbf{O})$ given by a Gaussian mixture model (GMM) with M-K-variate Gaussian components and diagonal covariance matrices for the state j, $j = 1, \ldots, Q$.

Commonly, HMM–GMM model parameters $\boldsymbol{\lambda}$ are iteratively estimated with the expectation–maximization (EM) algorithm (Dempster *et al* 1977, Rabiner 1989) using training data vectors; the *k-means* algorithm (Gersho and Gray 1993) is used for parameter initialization. A major disadvantage of the EM approach is that the number of Gaussian components M has to be determined *a priori*. Large M may result in a model that overfits the training data, whereas small M may result in models that are not accurate. In this study, a recursive greedy-EM algorithm is used where model parameters and the number of Gaussian components were estimated simultaneously using a Bayesian information criterion (Hu *et al* 2005). For HMMs with Q varying from 2 to 4, the number of Gaussian components M found via the greedy EM algorithm was found to be between 2 and 4 for different participants. It is interesting to note that such values are consistent with brain–computer interface studies based on HMMs (e.g. Sitaram *et al* 2007, Obermaier *et al* 2001).

The PA signals collected during baseline trials *performed in silence* (see section 2.2) were used to train HMMs for each of the six participants. Different HMM configurations were explored on a per-participant basis in order to allow for a user-centred approach due to the inter-subject variability resultant from external factors such as mental alertness, innate reflex reaction time, as well as familiarity with the procedure.

2.3.4. Automatic music imagery detection for body–machine interface control. Automatic music imagery detection was proposed as a means of developing control signals for body–machine interface usage. In order to detect music imagery events, PA signal temporal series $(\mathbf{O}(t)_{\text{test}})$ were computed from the imagery test trials described in section 2.2, with a running window of length L, and scored against the reference HMMs using a normalized likelihood measure

$$LH(l) = \Pr(\mathbf{O}(l)_{\text{test}}|\boldsymbol{\lambda}) = \frac{1}{L}\sum_{q}\pi_{q_0}\prod_{t=l}^{l+L-1} a_{q_{t-1},q_t} b_{q_t}(\mathbf{O}(t)_{\text{test}}), \quad (2)$$

where $l = 0, \ldots, T - L + 1$, T was the signal duration, window lengths ranging from $L =$ 1–15 s were explored and a window overlap of 0.33 s was used (i.e. LH was computed at a 3 Hz 'sample rate'). For numerical stability, the log-likelihood version of (2) was used in the simulations described in section 3. Different window lengths were explored to account for the user-specific latencies inherent to the physiological signals, which can range from 1 to 15 s (Kistler *et al* 1998).

Higher log-likelihood values suggested physiological responses similar to those observed during rest. Lower log-likelihood values, in turn, indicated deviations from such responses and were indicative of volitional mental activity. As such, a decrease in the likelihood function was expected during imagery periods and either an increase or a constant value was expected during the rest periods. A positive-to-negative slope change in the log-likelihood function was thus used to trigger candidate music imagery events. To compensate for possible motion artefacts that may produce a momentary positive-to-negative slope change, we imposed an additional criterion for the positive identification of music imagery, namely, that the negative slope must persist for at least 5 s. This limitation poses an upper bound on the system information transfer rate of 12 bits min^{-1}, which is somewhat lower than EEG-based BMIs, but still higher than those based on NIRS (van Gerven *et al* 2009). In summary, a music imagery event was detected at time n if

(i) $\text{sgn}(LH(n-1) - LH(n-2)) > 0$,
(ii) $\text{sgn}(LH(n) - LH(n-1)) < 0$ and
(iii) $(LH(n+P) - LH(n+P-1)) < 0$ for $P = 1, \ldots, 15$,

where 'sgn' represents the sign function. The plot in figure 3 depicts a representative $\log(LH)$ temporal series illustrating the expected increases during rest (unshaded) and decreases during music imagery (shaded), as well as the detected imagery segments (represented by the symbol '$\circ$').

2.3.5. Startle noise detection. The performance of mental tasks can be severely affected by ambient noise (e.g. Gumenyuk *et al* 2004, Cassidy and MacDonald 2007, Flaten *et al* 2005, Furnham and Strbac 2002). Moreover, physiological signals are sensitive to distracting auditory stimuli (Cook *et al* 1991); thus, it was expected that the body–machine interface performance would degrade when used in noisy environments. The log-likelihood temporal series computed for baseline data under startle noise conditions (see section 2.2), shown in figure 4, illustrates this behaviour. The sustained decreases in log-likelihood slopes, observed post-startle stimuli onset, would suffice to generate erroneous detection of 'imagery' events. In order to improve the system performance in practical environments, an airbourne microphone, combined with an acoustic energy thresholding based startle noise detection algorithm (described in detail elsewhere (Falk and Chan 2008)), was used to suppress erroneous activations resultant from involuntary startle-reflex responses.

Once acoustic startle noises are detected, erroneous detections due to startle reflexes need to be suppressed. As seen from figure 4, however, sustained decreases in $\log(LH)$ can have latencies of up to 7 s post-onset of a startle stimulus. Here, a simple compensation scheme was explored; activations that started within 5 s (empirically set based on pilot experiments) post-startle detection were suppressed. On the other hand, if a startle was detected after a

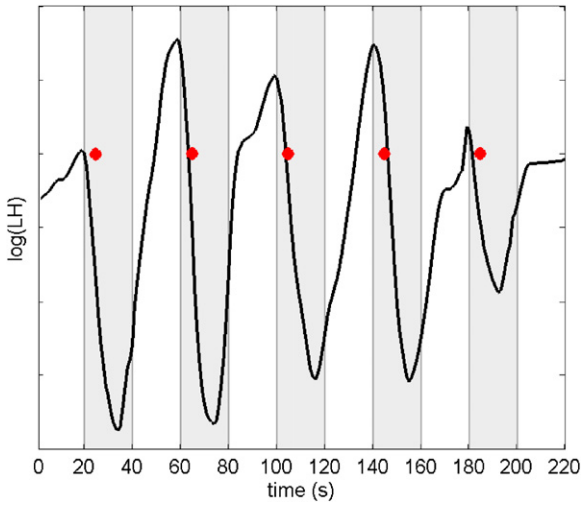

Figure 3. Log-likelihood temporal series computed from the test data consisting of alternating rest (unshaded regions) and imagery (shaded) periods. The circles represent correctly detected music imagery events.

sustained decrease in $\log(LH)$ had been observed for at least 2.5 s, suppression did not occur as it was assumed that music imagery was already being performed.

2.4. System evaluation: performance metrics

To objectively quantify the system performance, sensitivity and specificity were used as performance metrics. The measures are given by

$$\text{Sensitivity} = \frac{\text{TP}}{\text{TP} + \text{FN}} \times 100\%, \tag{3}$$

$$\text{Specificity} = \frac{\text{TN}}{\text{TN} + \text{FP}} \times 100\%, \tag{4}$$

where FP and FN denote the number of false positives and false negatives, respectively; TP and TN, in turn, represent the number of true positives and true negatives. Sensitivity is related to the percentage of correctly detected imagery events. Specificity, on the other hand, is related to the percentage of correctly detected rest intervals. Specificity values close to unity indicated that erroneous detections seldom occurred; in the context of startle noise compensation, it indicated that erroneous interface activations had been correctly suppressed.

For the developed body–machine interface, TP are defined as correctly detected activations which occurred within 7.5 s post-transition from rest to imagery. This grace period accounts for the participant reaction time, i.e. delay in initiating music imagery and the response latency associated with the physiological signals under consideration. FP are defined as erroneously detected activations which occur during rest intervals. FN, in turn, account for genuine activations that are not detected during imagery and TN account for correctly classified rest periods.

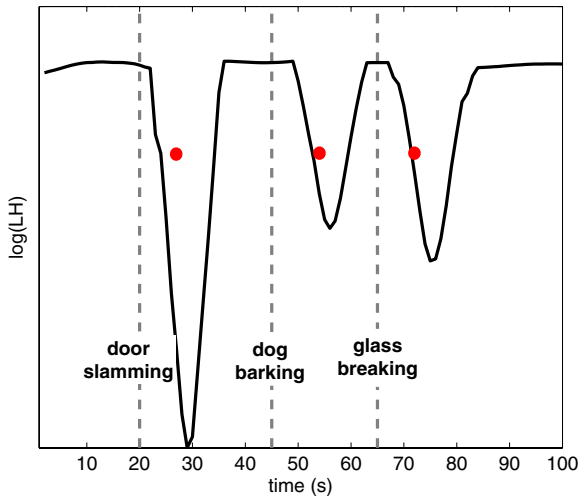

Figure 4. Log-likelihood temporal series computed from baseline data (*without* music imagery) in the presence of three startle stimuli. The circles represent erroneously detected music imagery events.

3. Experimental results

This section reports the contribution of each signal and the overall performance obtained under silent and noisy conditions.

3.1. Gauging signal contributions

As mentioned previously, normalized mutual information (I_{norm}) was used to gauge the contribution of each PA signal to imagery detection. Table 1 reports I_{norm} between each of the four PA signals under consideration and the stimulus pattern depicted in figure 1; signals with larger I_{norm} correspond to signals which contributed more to imagery detection. As can be seen, EDA and ST were the two modalities which contributed the most to imagery detection for all six participants; half the participants had EDA as their major contributor, a finding that resonates with those reported in Blain *et al* (2006, 2008b). Conversely, all participants had RR as the signal that contributed the least; a similar finding has been reported in the polygraph literature (Ben-Shakhar and Dolev 1996).

Moreover, the graph depicted in figure 5 shows the system specificity and sensitivity values obtained under controlled silent conditions for the increasing number of PA signals used to train the subject-specific HMMs. When using only the signal that attained the highest I_{norm}, the average sensitivity and specificity values of 35% and 58.3% were attained, respectively. Performance increased monotonically as more signals were incorporated, thus suggested that complex signal interactions due to the cognitive task were being captured by the HMMs. Once all signals were used, the average sensitivity and specificity of 94.2% and 93.3% were attained, respectively.

In order to improve usability, user-centred designs (UCDs) are commonly explored (Abras *et al* 2004). Here, UCD was achieved by selecting optimal HMM configurations (i.e. Q and M parameters) and window sizes L for each participant. Table 2 reports such parameters for each individual. Throughout the course of the task interval, the participants likely did not transition

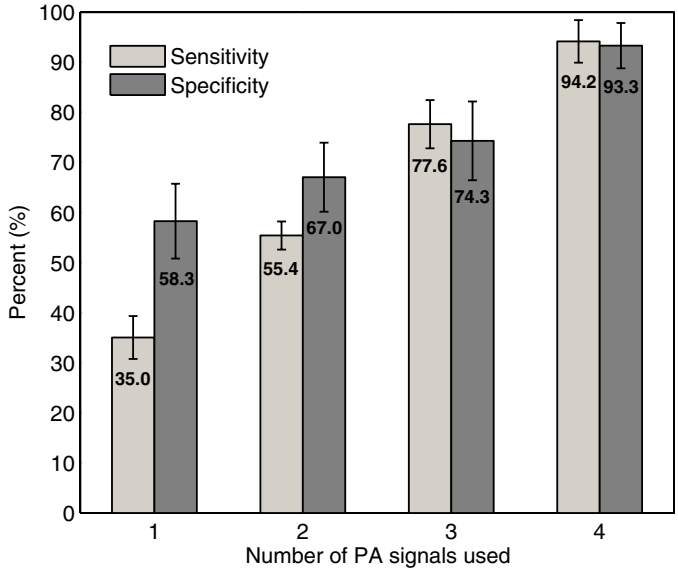

Figure 5. System sensitivity and specificity obtained under silent conditions for the increasing number of PA signals used to train the HMMs.

Table 1. Normalized mutual information (I_{norm}) between each of the four PA signals under consideration and the stimulus pattern depicted in figure 1. The signal with largest I_{norm} corresponds to the signal which contributes the most to imagery detection.

	Contribution order (I_{norm})			
Subject	First	Second	Third	Fourth
1	ST (0.62)	EDA (0.61)	HR (0.41)	RR (0.36)
2	ST (0.64)	EDA (0.59)	HR (0.47)	RR (0.33)
3	EDA (0.62)	ST (0.60)	HR (0.46)	RR (0.34)
4	EDA (0.62)	ST (0.59)	HR (0.45)	RR (0.36)
5	EDA (0.61)	ST (0.52)	HR (0.48)	RR (0.34)
6	ST (0.60)	EDA (0.59)	HR (0.45)	RR (0.33)

immediately from a rest state to an active music imagery state; this was likely the reason for HMMs with four states being selected for the majority of the participants. Nonetheless, for two participants (subjects 3 and 4), HMMs with two states were deemed optimal, suggesting the sharper transition between the two mental states. For the same participants, shorter window lengths were deemed optimal, hence corroborating the assumption of faster reaction times.

For practical applications, a 'calibration' session with known imagery and rest intervals is needed in order to optimize system parameters. Similar to calibration sessions required by existing speech recognizers, this can be achieved with minimal third-party intervention. Moreover, since the proposed system requires only *baseline* (rest) information for HMM training, such calibration sessions can be performed in the order of tens of seconds, and are thus unlikely to pose a serious burden on the user. The optimal system parameters reported in table 2 were used to estimate the performance measures in figure 5 for silent conditions, as well as those reported in section 3.2 for noisy conditions.

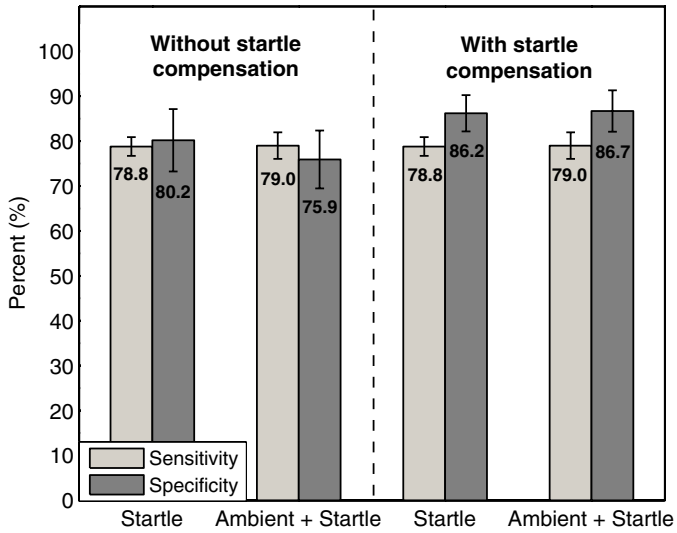

Figure 6. System sensitivity and specificity obtained under noisy conditions with and without startle noise detection and compensation.

Table 2. Optimal HMM parameters and $\log(LH)$ window lengths L obtained for each participant.

Subject	Q	M	L (s)
1	4	2	9
2	4	2	7
3	2	4	6
4	2	4	6
5	4	3	10
6	4	3	8

3.2. System performance under noisy conditions

The graph in figure 6 shows the system specificity and sensitivity when the interface was used under noisy conditions, both with and without startle noise detection/compensation. Relative to silent conditions, a decrease of approximately 16% was observed in system sensitivity under noisy conditions *without* startle noise compensation. In terms of specificity, the decreases of 14% and 19% were observed for startle only and combined startle–ambient noise scenarios, respectively. Once startle noise compensation was in place, the system specificity only decreased by approximately 7% relative to silent conditions for both startle only and combined startle–ambient noise scenarios. Such performance levels were not significantly different ($p > 0.5$, t-test) from those observed in controlled silent environments.

4. Conclusions

This paper investigated the use of four non-invasively acquired physiological signals, namely EDA, ST, HR and RR, as access channels for the control of body–machine interfaces. Subject-specific HMMs of the normative physiological response during rest (baseline) were

used to automatically detect volitional physiological changes due to a music imagery task. Experiments with six able-bodied adults resulted in the average sensitivity and specificity values of 94.2% and 93.3%, respectively, in controlled silent environments. Under noisy conditions, the proposed system equipped with a startle noise detection and compensation scheme achieved specificity levels similar to those attained in silence. These results are encouraging and warrant future investigations on the use of HMMs and PA signals for body–machine interface research.

Acknowledgments

This study was funded by the Natural Sciences and Engineering Research Council of Canada, the Ward Family Foundation and the Canada Research Chair program.

References

Abras C, Maloney-Krichmar D and Preece J 2004 User-centered design *Encyclopedia of Human–Computer Interaction* (Thousand Oaks, CA: Sage)

Alsayegh O A 2000 EMG-based human-machine interface system *Proc. IEEE Int. Conf. on Multimedia and Expo, 2000. ICME 2000* vol 2

Ben-Shakhar G and Dolev K 1996 Psychophysiological detection through the guilty knowledge technique: effects of mental countermeasures *J. Appl. Psychol.* **81** 273–81

Blain S, Chau T and Mihailidis A 2008a Peripheral autonomic signals as access pathways for individuals with severe disabilities: a literature appraisal *Open Rehabil. J.* **1** 27–37

Blain S, Mihailidis A and Chau T 2006 Conscious control of electrodermal activity: the potential of mental exercises *Proc. Int. Conf. IEEE Engineering in Medicine and Biology Society*

Blain S, Mihailidis A and Chau T 2008b Assessing the potential of electrodermal activity as an alternative access pathway *Med. Eng. Phys.* **30** 498–505

Cassidy G and MacDonald R A R 2007 The effect of background music and background noise on the task performance of introverts and extraverts *Psychol. Music* **35** 517–37

Chen Y L 2001 Application of tilt sensors in human-computer mouse interface for people with disabilities *IEEE Trans. Neural Syst. Rehabil. Eng.* **9** 289–94

Cook E W, Hawk L W, Davis T L and Stevenson V E 1991 Affective individual differences and startle reflex modulation *J. Abnormal Psychol.* **100** 5–13

Dempster A P, Laird N M and Rubin D B 1977 Maximum likelihood from incomplete data via the EM algorithm *J. R. Stat. Soc. Ser. B* **39** 1–38

Falk T H and Chan W Y 2008 Hybrid signal-and-link-parametric speech quality measurement for VoIP communications *IEEE Trans. Audio, Speech Language Processing* **16** 1579–89

Flaten M, Nordmark E and Elden A 2005 Effect of background noise on the human startle reflex and prepulse inhibition *Psychophysiology* **42** 298–305

Furnham A and Strbac L 2002 Music is as distracting as noise: the differential distraction of background music and noise on the cognitive test performance of introverts and extraverts *Ergonomics* **45** 203–17

Gersho A and Gray R 1993 *Vector Quantization and Signal Compression* (Dordrecht: Kluwer)

Gumenyuk V, Korzyukov O, Alho K, Escera C and Naatanen R 2004 Effects of auditory distraction on electrophysiological brain activity and performance in children aged 8–13 years *Psychophysiology* **41** 30–6

Hu R, Li X and Zhao Y 2005 Acoustic model training using greedy EM *Proc. Int. Conf. Acoustics, Speech, and Signal Processing* vol 1 pp 697–700

Kistler A, Mariauzouls C and von Berlepsch K 1998 Fingertip temperature as an indicator for sympathetic responses *Int. J. Psychophysiol.* **29** 35–41

Kvalseth T 1987 Entropy and correlation: some comments *IEEE Trans. Syst. Man Cybern.* **17** 517–9

Memarian N, Venetsanopoulos A N and Chau T 2009 Infrared thermography as an access pathway for individuals with severe motor impairments *J. NeuroEng. Rehabil.* **6** 11

Obermaier B, Guger C, Neuper C and Pfurtscheller G 2001 Hidden Markov models for online classification of single trial EEG data *Pattern Recognit. Lett.* **22** 1299–309

Rabiner L 1989 A tutorial on hidden Markov models and selected applications in speech recognition *Proc. IEEE* **77** 257–86

Roy D M, Panayi M, Erenshteyn R, Foulds R and Fawcus R 1994 Gestural human-machine interaction for people with severe speech and motor impairment due to cerebral palsy *Proc. Conf. on Human Factors in Computing Systems* pp 313–14

Sesin A, Adjouadi M, Ayala M, Cabrerizo M and Barreto A 2008 Eyeing a real-time human-computer interface to assist those with motor disabilities *IEEE Potentials* **27** 19–25

Sitaram R, Zhang H, Guan C, Thulasidas M, Hoshi Y, Ishikawa A, Shimizu K and Birbaumer N 2007 Temporal classification of multichannel near-infrared spectroscopy signals of motor imagery for developing a brain-computer interface *NeuroImage* **34** 1416–27

Struijk L 2006 An inductive tongue computer interface for control of computers and assistive devices *IEEE Trans. Biomed. Eng.* **53** 2594–7

Su M C and Chung M T 2001 Voice-controlled human-computer interface for the disabled *Comput. Control Eng. J.* **12** 225–30

Tsukahara R and Aoki H 2002 Skin potential response in letter recognition task as an alternative communication channel for individuals with severe motor disability *Clinical Neurophysiol.* **113** 1723–33

van Gerven M *et al* 2009 The brain-computer interface cycle *J. Neural Eng.* **6** 041001

Wilhelm B, Jordan M and Birbaumer N 2006 Communication in locked-in syndrome: effects of imagery on salivary pH *Neurology* **67** 534